From the above data it appears that introducing a methyl group between the two methyls results in a considerable increase of the $\zeta$ effect.

The splitting of the high-field component in the methyl signal in sample V could be attributed to the effect of the steric pentads. However, this hypothesis shall be tested in further investigation.

Finally the methylene $C_{2,4}$ absorption was affected by the diad and triad configuration as recently reported in the literature.[20]

## IV. Conclusions

The results of the present work show that the microstructure of polymers having monomer units with a length of four atoms can be determined by $^{13}C$ NMR spectroscopy. Long-range steric effects observed on the methyl group of both saturated and unsaturated polymers allow a measurement of the tacticity index. This nondestructive determination of tacticity avoids cumbersome chemical treatments such as hydrogenation or oxidative cleavage.

The chemical shift of the methyl signals due to the different steric sequences in poly(1-methyltetramethylene), i.e., $\delta_{mm} > \delta_{mr} > \delta_{rr}$, is inverted by introducing double bonds in the polymer chain both in cis and trans polypentadienes, i.e., $\delta_{rr} > \delta_{mr} > \delta_{mm}$.

This would suggest that, although the effect of the $\zeta$ substituent is stereospecific and additive both in hydrogenated and unsaturated polymers, the introduction of double bonds in the polymer chain changes the numerical values of the additive parameters for the meso and racemic $\zeta$ substituent.

The double bonds also slightly affect the CH absorption by removing the degeneracy observed in the saturated polymer.

## References and Notes


(1) D. M. Grant and E. G. Paul, *J. Am. Chem. Soc.*, **86**, 2984 (1964).
(2) L. P. Lindeman and J. C. Adams, *Anal. Chem.*, **43**, 1245 (1971).
(3) D. K. Dalling and D. M. Grant, *J. Am. Chem. Soc.*, **89**, 6612 (1967).
(4) F. A. Bovey, "High Resolution NMR of Macromolecules", Academic Press, New York, N.Y., 1972.
(5) S. Boileau, H. Cheradame, W. Lapeyre, L. Sousselier, and P. Sigwalt, *J. Chem. Phys.*, **70**, 879 (1973).
(6) N. Oguni, K. Lee, and H. Tani, *Macromolecules*, **5**, 819 (1972).
(7) L. F. Johnson, *Anal. Chem.*, **43**, 28/A (1971).
(8) A. Zambelli, D. E. Dorman, A. I. R. Brewster, and F. A. Bovey, *Macromolecules*, **6**, 925 (1973).
(9) A. Zambelli, P. Locatelli, G. Bajo, and F. A. Bovey, *Macromolecules*, **8**, 687 (1975).
(10) A. Provasoli and D. Ferro, *Macromolecules*, **10**, 874 (1977).
(11) G. Natta, L. Porri, P. Corradini, and G. Zanini, *J. Polym. Sci.*, **51**, 463 (1961).
(12) G. Natta, L. Porri, A. Carbonaro, F. Ciampelli, and G. Allegra, *Makromol. Chem.*, **51**, 229 (1962).
(13) G. Natta, L. Porri, G. Stoppa, G. Allegra, and F. Ciampelli, *J. Polym. Sci., Part B*, **1**, 67 (1963).
(14) G. Gatti and A. Carbonaro, *Makromol. Chem.*, **175**, 1627 (1974).
(15) G. Audisio and A. Silvani, *J. Chem. Soc., Chem. Commun.*, 482 (1976).
(16) M. Farina, U. Pedretti, M. T. Gramegna, and G. Audisio, *Macromolecules*, **3**, 475 (1970).
(17) G. Natta, L. Porri, A. Carbonaro, and G. Stoppa, *Makromol. Chem.*, **77**, 114 (1967).
(18) L. Porri, D. Corato, and G. Natta, *Eur. Polym. J.*, **5**, 1 (1969).
(19) L. A. Mango and R. W. Lenz, *Makromol. Chem.*, **163**, 13 (1973).
(20) K. F. Elgert and W. Ritter, *Makromol. Chem.*, **178**, 2857 (1977).


# Compatibility in $PVF_2$/PMMA and $PVF_2$/PEMA Blends as Studied by Pulsed NMR


**D. C. Douglass‡ and V. J. McBrierty***

*Bell Laboratories, Murray Hill, New Jersey 07974, and Physical Laboratory, Trinity College, Dublin, Ireland.*

*Received September 13, 1977*


ABSTRACT: The transient Overhauser effect in blends of $PVF_2$ and PMMA has been exploited to provide information on the degree of mixing of the two component polymers. Based upon the conviction that cross-relaxation effects imply near-neighbor dipolar interactions between protons and fluorine nuclei, the cross-relaxation data, supported by $T_{1\rho}$ and $T_2$ measurements, indicate that a substantial fraction of the two component polymers are intimately mixed in the amorphous regions. There are indications of premelting in the blends. Similar conclusions apply to $PVF_2$/PEMA blends.


Several recent studies[1-12] have demonstrated compatibility between certain polymer pairs over a wide range of blend composition. The extent to which compatibility exists has been decided according to criteria such as the transparency of the blend, consideration of the solubility parameters involved, and transition temperatures in the blend, in particular the glass transition temperature $T_g$.[6] Recently, the degree of polarization of the longitudinal Brillouin peaks has been used as a sensitive measure of compatibility.[13] Molecular weight, tacticity, and blend composition are factors which influence, in a crucial way, the ultimate compatibility achieved. For example, isotactic PMMA forms an incompatible system with PVC while syndiotactic PMMA and PVC are compatible.[6]

Even though two polymers are deemed compatible it remains to determine the topology, graininess, or homogeniety, or whatever other term appropriately characterizes the blend structure. Different experiments, such as microscopy, light scattering, NMR, and X-ray diffraction, examine this structure over decreasing characteristic lengths and combine to generate a composite picture of the blend structure. This paper presents NMR data, sensitive to short-range interactions, which emphasize results obtained from cross-relaxation experiments designed to augment line width and spin–lattice relaxation experiments and to circumvent complexities sometimes resulting from spin diffusion.[7,10,11]

The materials chosen for study are blends of poly(vinylidine fluoride)/poly(methyl methacrylate) ($PVF_2$/PMMA) and poly(vinylidine fluoride)/poly(ethyl methacrylate) ($PVF_2$/PEMA) blends of different composition which have received much attention of late by other methods.[12-14] In many respects these blends are particularly suited to study by pulsed NMR since preliminary experiments on the component polymers have been performed[11,15,16] and, additionally, cross-relaxation between the two unlike $^1H$ and $^{19}F$ spin sys-


‡ Bell Laboratories.
* Trinity College.


0024-9297/78/2211-0766$01.00/0 

tems provides a sensitivity in certain relaxation measurements which is not otherwise available.[11]

## Experimental Section

**Sample Materials. $PVF_2$:** The $PVF_2$ resin, in powder form, was supplied by Pennwalt Corp. under the trade name Kynar 821. The molecular weight characteristics are $M_n = 2.1 \times 10^5$ and $M_w = 4 \times 10^5$.[13]

**$PVF_2$/PMMA:** The two blends studied, 75/25 (Kynar RC3335A) and 40/60 (Kynar RC 3335B) by weight, were obtained commercially from the Pennwalt Corp. These mixtures were compounded from Kynar 301 $PVF_2$ resin ($M_n = 1.1 \times 10^5$, $M_w = 3.8 \times 10^5$) and Acrylite B115 PMMA resin ($M_n = 3.7 \times 10^4$, $M_w = 9.2 \times 10^4$) supplied by American Cyanamid.[13] Samples were annealed for 5 h at 110 °C and cooled to room temperature in the oven over a period of 5 h.

**PMMA:** The PMMA used was Acrylite H-12 supplied by American Cyanamid with similar characteristics to Acrylite B115.

**$PVF_2$/PEMA:** Mixtures were blended in ratios of 80/20 and 40/60 by weight in a Brabender mixer at 180 °C, for about 10 min. The blend was subsequently molded into sheets at ~150 °C in a press and then quenched in air.

**PEMA:** The measured viscosity in 2-butanone at 23 °C was $[\eta] = 0.75$ which provided $M_v = 4.0 \times 10^5$ using establishing formulas.[17]

All samples were evacuated in NMR tubes at room temperature for a period of 24 h.

## Spectrometer and Data Nalaysis

Two types of resonance experiment were performed, one involving conventional $T_1$, $T_{1\rho}$, and $T_2$ measurements and the other cross-relaxation effects.

In the measurement of $T_1$, $T_{1\rho}$, and $T_2$ the basic spectrometer[18] was interfaced, via a Biomation 610 digitizer, to a Nicolet 1072 signal averager. The recovery time of the spectrometer following a sequence of pulses was ~6 μs and a 90° pulse was of 2 μs duration.

The solid echo sequence,[19] 90°–$\tau$–90° (90° phase shift), provided an approximation to the complete free induction decay from which $T_2$ was measured as $t_{1/2}/\ln 2$ where $t_{1/2}$ is the time taken for the signal to decay to half the initial intensity. The analysis of composite $T_2$ decays has been discussed earlier.[20] The 180°–$\tau$–90° pulse sequence[21] was used to obtain $T_1$. Where nonexponential behavior was evident from a change in shape of the decay for successive $\tau$ values the components were extracted from plots of $\log [M_0 - M(\tau)]/2M_0$ vs. $\tau$, where $M_0$ is the fully recovered magnetization ($\tau \to \infty$). $T_{1\rho}$ was obtained from the 90°–90° phase-shift spin-locking sequence[22] and decays were analyzed in terms of two components where appropriate. Data were recorded for $H_1 = 25G$ in order to facilitate comparison with earlier results of $PVF_2$.[16]

Cross-relaxation effects between the $^1H$ and $^{19}F$ spin systems were measured by the transient Overahuser experiment.[11,23] This required the application of a 180° pulse at $t = 0$, at the resonant frequency of the hydrogen spins, and a subsequent 90° pulse for the fluorine spins at a variable time $t$. This was achieved with a crossed coil probe, one coil being tuned to fluorine resonance (30 MHz) and the other to proton resonance (31.888 MHz). Owing to the rather long $\pi$ pulse length for proton resonance (18 μs), a single coil probe system which provided a proton $\pi$ pulse of ~5 μs was used to examine again data obtained in the cross-coil system in the crucial temperature region −40 to +25 °C. Results were generally in good agreement with some tendency for the shorter $\pi$ pulse to give slightly larger $\sigma$ values, as one might expect.[11]

At each temperature, $(I_z - I_0)/S_0$ ($I$ refers to fluorine and $S$ to proton magnetization, respectively) was plotted against $t$, the time between the 180 and 90° pulses, in the manner described previously.[11] In all cases a decrease in the $^{19}F$ signal intensity was observed. In contrast to the earlier experiment on $PVF_2$, the direct relaxation parameters $\rho$ and $\rho'$[23] are no longer equal in the blends since there are different numbers of $^1H$ and $^{19}F$ nuclei now present. In this case the experimental plot of $(I_z - I_0)/S_0$ vs. $t$ requires a more general analysis. In addition to the considerations which lead to the use of the Block equations to describe cross-relaxation, as discussed in the earlier paper on $PVF_2$,[11] we assume that spin diffusion distributes energy among all nuclei of any one type rapidly compared to the rate of cross-relaxation. The Block equations retain a simple form[23] (see Appendix I)

$$\frac{d(I - I_0)}{dt} = -\rho(I - I_0) - \sigma(N_I/N_S)(S - S_0) \qquad (1)$$

$$\frac{d(S - S_0)}{dt} = -\rho'(S - S_0) - \sigma(I - I_0)$$

where $\sigma = \Sigma_{ij}\, \sigma_{ij}/N_F$ is defined so that it is a mean rate for cross-relaxation of fluorine nuclei, $\rho$ and $\rho'$ retain their usual significance in characterizing spin–lattice relaxation, and $N_i$ is the number of nuclei of type i. Thus

$$\frac{I_Z - I_0}{S_0} = \frac{2\sigma}{[(\rho - \rho')^2 + 4\bar{\sigma}^2]^{1/2}} \left\{ e^{-[\rho+\rho'+[(\rho-\rho')^2+4\bar{\sigma}^2]^{1/2}]t/2} - e^{-[\rho+\rho'-[(\rho-\rho')2+4\bar{\sigma}^2]^{1/2}]t/2} \right\} \qquad (2)$$

where $\bar{\sigma} = (N_F/N_H)^{1/2}\sigma$. The curve-fitting procedure used to obtain $\rho$, $\rho'$, and $\sigma$ is based upon the method described by Hamming[24] for the analysis of multiexponential functions. The details pertinent to our requirements are given in Appendix II.

Inspection of eq 1 shows that it is not possible, without additional information, to assign $\rho$ or $\rho'$ to one or the other of the nuclear spin systems.

## Results

An understanding of NMR relaxation in the blends rests upon prior knowledge of the NMR response in the component polymers. Figure 1 summarizes the $^{19}F$ $T_1$, $T_{1\rho}$, and $T_2$ relaxation data for $PVF_2$ (crystal form II) as reported in detail

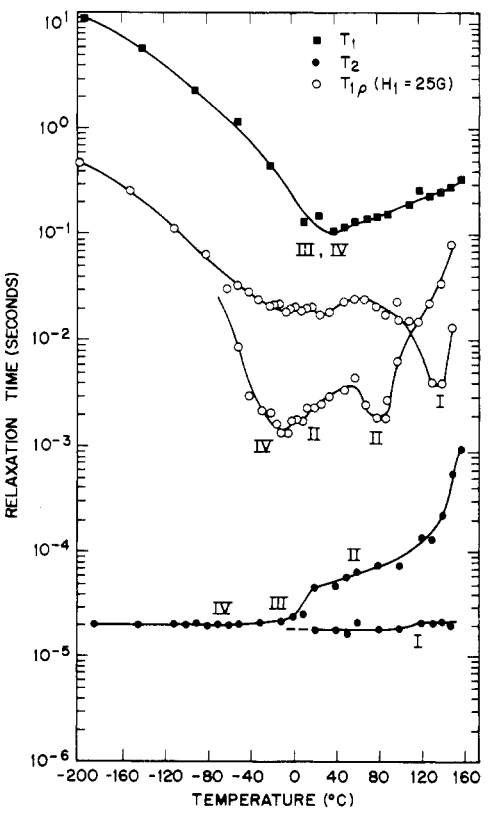


**Figure 1.** $T_1$, $T_2$, and $T_{1\rho}$ data for $^{19}F$ resonance in $PVF_2$ as a function of temperature. I–IV signify the relaxation processes as given in Table I.

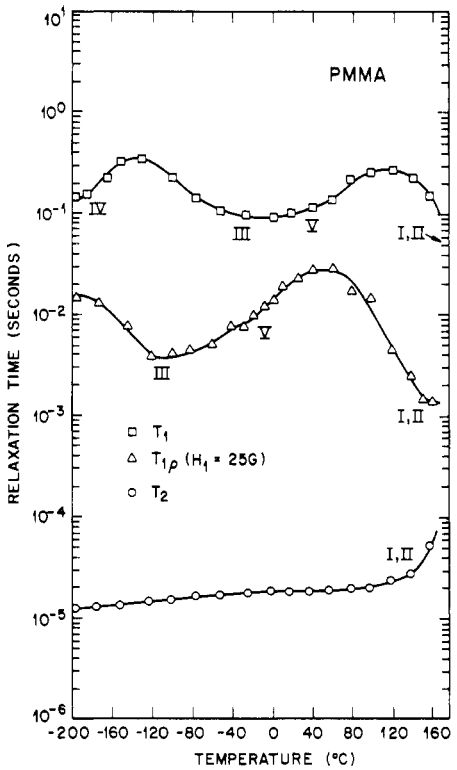


**Figure 2.** $T_1$, $T_2$, and $T_{1\rho}$ data for $^1H$ resonance inPMMA as a function of temperature. I–V signify the relaxation processes as given in Table I.

in an earlier paper.[16] Figures 2 and 3 show our recorded $^1H$ data for PMMA and PEMA. The molecular processes which have been assigned to the various relaxations are summarized in Table I.[15,16,25] A feature of the PMMA data which merits comment is the shoulder in the $T_{1\rho}$ curve at −30 °C. This is probably a manifestation of the process reponsible for the $T_1$

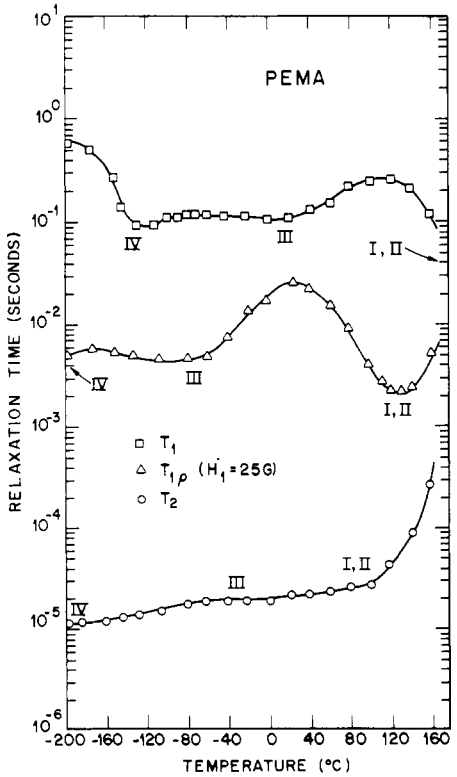


**Figure 3.** $T_1$, $T_2$, and $T_{1\rho}$ data for $^1H$ resonance in PEMA as a function of temperature. I–IV signify the relaxation processes as given in Table I.

**Table I**
**Molecular Motional Assignments to Relaxation Processes in $PVF_2$, PMMA, and PEMA as Observed in Figures 1–3**

| Polymer | Relaxation | Molecular process | Ref |
|---|---|---|---|
| $PVF_2$ | I ($\alpha$) | Crystalline chain rotation or oscillation | 16 |
| | II ($\beta'$) | Motion of folds | 16 |
| | III ($\beta$) | General motion of amorphous chains | 16 |
| | IV ($\gamma$) | Restricted motion (possibly rotation) of amorphous chains | 16 |
| PMMA | I ($\alpha$) | Glass transition | 15 |
| PEMA | II ($\beta$) | Motion of ester side groups | 15 |
| | III | Motion of main chain methyl groups | 15 |
| | IV | Motion of side chain methyl groups (or possibly the whole group in PEMA) | 15 |
| | V (PMMA only) | Torsional motion of main chain | 25 |

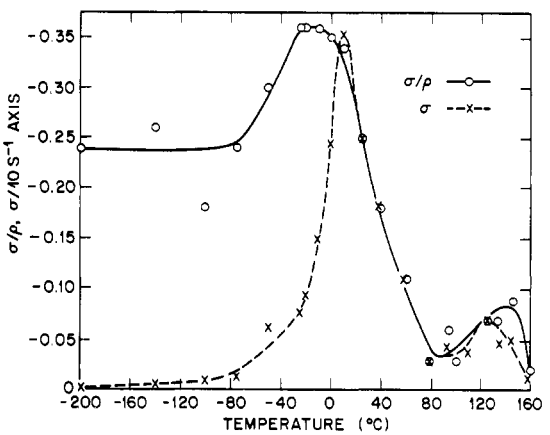


**Figure 4.** Variation of $\sigma$ and $\sigma/\rho$ with temperature for pure $PVF_2$.

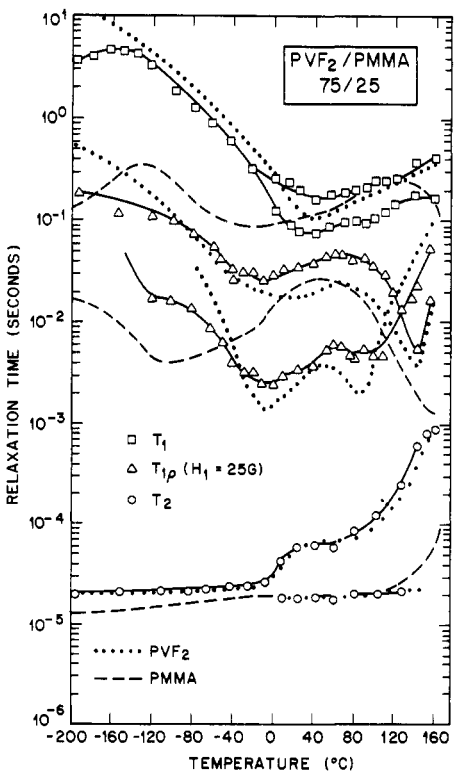


**Figure 5.** $T_1$, $T_2$, and $T_{1\rho}$ data for the 75/25 $PVF_2$/PMMA blend: ··· and - - - denote the $PVF_2$ and PMMA response, respectively.

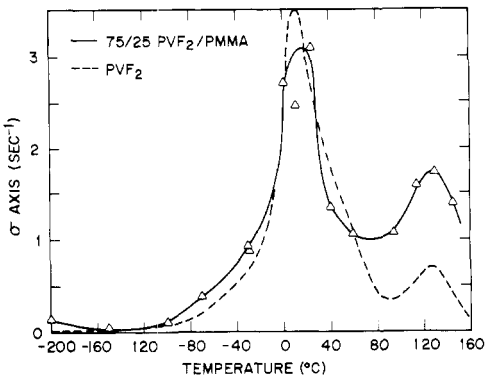


**Figure 6.** Temperature variation of $\sigma$ for the 75/25 $PVF_2$/PMMA blend. The variation in pure $PVF_2$ (dashed curve) is included for comparison.

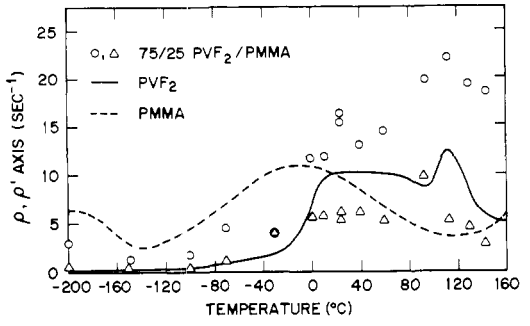


**Figure 7.** Temperature dependence of the two $\rho$'s, determined from eq 1, for the 75/25 $PVF_2$/PMMA blend. $\rho$ for $PVF_2$ (solid line) and PMMA (dashed line) are included for comparison.

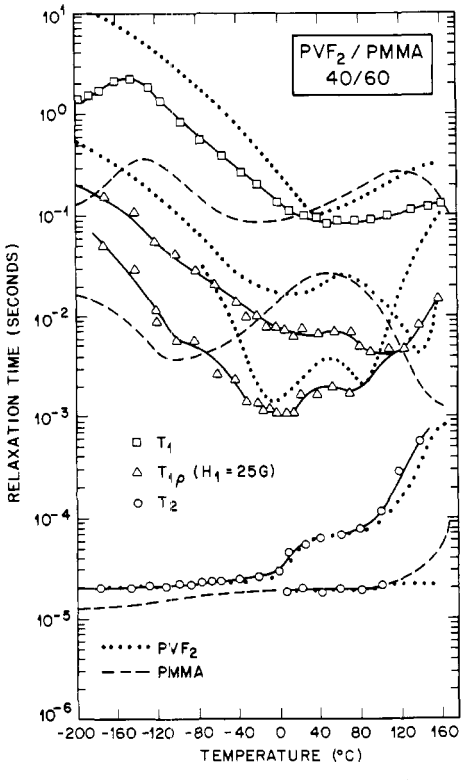


**Figure 8.** $T_1$, $T_2$, and $T_{1\rho}$ data for the 40/60 $PVF_2$/PMMA blend: ··· and - - - denote the $PVF_2$ and PMMA response, respectively.

miminum at 50 °C observed by Slichter in poly(methyl $\alpha$-fluoroacrylate) and also considered to be present in PMMA as an unresolved minimum.[25] Slichter has suggested torsional motions of the main chain for this relaxation.

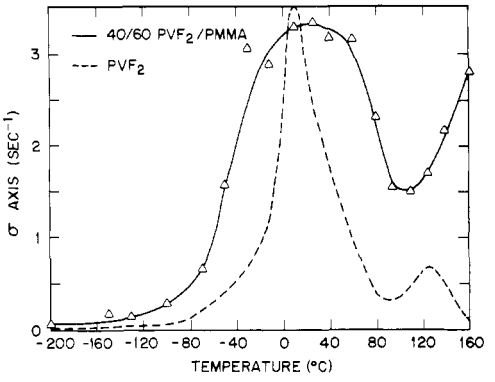


**Figure 9.** Temperature variation of $\sigma$ for the 40/60 $PVF_2$/PMMA blend. The variation in pure $PVF_2$ (dashed curve) is included for comparison.

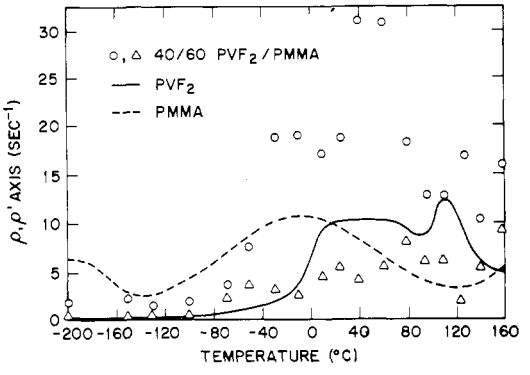


**Figure 10.** Temperature dependence of the two $\rho$'s, determined from eq 1, for the 40/60 $PVF_2$/PMMA blend. $\rho$ for $PVF_2$ (solid line) and PMMA (dashed line) are included for comparison.

The cross-relaxation data for $PVF_2$, taken from ref 11, are presented in Figure 4.

**$PVF_2$/PMMA Blends.** In Figures 5 through 10 the various NMR data are plotted as a function of temperature for the $PVF_2$/PMMA blends. Where required, the results for component polymers are included for comparison. While this composite picture is complex it is the comparison of component and blend results which makes the substance of our discussion and therefore this format is considered most useful.

**$T_1$ Relaxation Data.** At low temperatures the $^{19}F$ $T_1$ data for the $PVF_2$/PMMA blends show a marked sensitivity, in the form of a minimum, to the presence of the low-temperature minimum in the $^1H$ resonance results for PMMA. This is evidence for an interaction between the protons of the PMMA and the fluorines in $PVF_2$ which one would expect in either a phase-separated system where spin diffusion is effective or in a solid solution. The effect increases with PMMA content. For the 75/25 blend at temperatures in excess of ca. −20 °C two $T_1$ components are observed.

**$T_{1\rho}$ Relaxation Data.** The important characteristics in the $^{19}F$ $T_{1\rho}$–temperature curves for $PVF_2$/PMMA follow: (i) The short, amorphous, $T_{1\rho}$ component in both the 75/25 and 40/60 blends exhibits a minimum at ca −110 °C, the temperature at which the minimum for main chain methyl group motion occurs in PMMA. As with the $T_1$ data, the depth of the $^{19}F$ resonance minimum increases with PMMA content. (ii) Compared with $PVF_2$, all minima are shallower in the 75/25 blend. (iii) The magnitudes of the crystalline and amorphous $T_{1\rho}$ components are shorter over the complete temperature range in the 40/60 blend as compared with $PVF_2$. Furthermore, above ~65 °C exponential $T_{1\rho}$ decay is observed and there is no evidence of a well-defined $\alpha$-relaxation minimum.

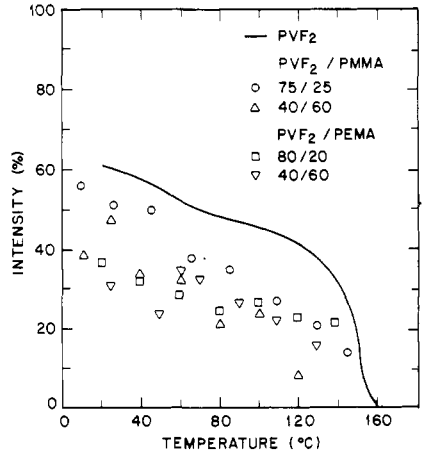


**Figure 11.** The intensity of the short $T_2$ component as a function of temperature for the blends. The solid line represents the $PVF_2$ response.

**$T_2$ Relaxation Data.** Two aspects of the $^{19}F$ $T_2$ data are especially worthy of note. Although not evident from the figures, $T_2$ for the two blends is slightly greater than for neat $PVF_2$ over the temperature range ca. −140 to ~0 °C. $T_2$ for PMMA correspondingly increases within this temperature range, principally as a result of the onset of main chain methyl motions. The second point relates to the temperature at which the short $T_2$ component disappears: +100 and +130 °C respectively in the 40/60 and 75/25 $PVF_2$/PMMA blends, as compared with ~150 °C in $PVF_2$.

**Cross-Relaxation Data.** The variation with temperature of the cross-relaxation parameter $\sigma$ for the blends is similar to that observed in $PVF_2$. In the 40/60 material, however, the maximum in the vicinity of room temperature is markedly broader than in either the 75/25 blend or the neat $PVF_2$. In addition, the higher temperature peak is not attained below the melting point. At high temperatures, $\sigma$ for both blends is greater than that observed in $PVF_2$.

At temperatures below ca. −20 °C $\rho$ and $\rho'$ are intermediate between $\rho$ for $PVF_2$ and $\rho$ ($= T_1^{-1}$) for PMMA. At higher temperatures one of the two $\rho$'s for the blends is much greater in magnitude than $\rho$ for either of the component polymers.

**Component Intensity Data.** In Figure 11 the intensity of the short, crystalline, $T_2$ component for the blends is presented as a function of temperature and compared with the corresponding data for $PVF_2$.[16] The scatter in the data for the blend with low $PVF_2$ content reflects the difficulty in resolving two components in this material owing to the inferior signal-to-noise ratio in the $^{19}F$ free-induction decay. The data indicate crystallinities for the $PVF_2$ component of about 35 and 25% in the 75/25 and 40/60 $PVF_2$/PMMA samples, respectively.

The intensity of the long $T_{1\rho}$ component for the blends displayed the same complex behavior with temperature as was observed in $PVF_2$[16] and will not be discussed herein.

**$PVF_2$/PEMA Blends.** Figures 12 and 13 contain the $T_1$, $T_2$, and $T_{1\rho}$ data for the $PVF_2$/PEMA blends. In most all respects the behavior is similar to $PVF_2$/PMMA. In the 80/20 sample, however, nonexponential $T_1$ decay is confined to the region of the minimum. Furthermore, in the $T_{1\rho}$ data for this blend, the two $T_{1\rho}$ components do not cross over at temperatures in the vicinity of +110 °C; rather, the shorter $T_{1\rho}$ tends to reflect the PEMA behavior as temperatures approach the melting point. In the $T_2$ data for both $PVF_2$/PEMA blends the short $T_2$ persists almost to the same temperature as in $PVF_2$. $T_2$ (and $T_{1\rho}$) component intensity data follow the same pattern with temperature as is observed with $PVF_2$/PMMA. No cross-relaxation data were recorded for these blends but it is to be expected that the response in $PVF_2$/PMMA should provide a reasonable indicator of the behavior in $PVF_2$/PEMA.

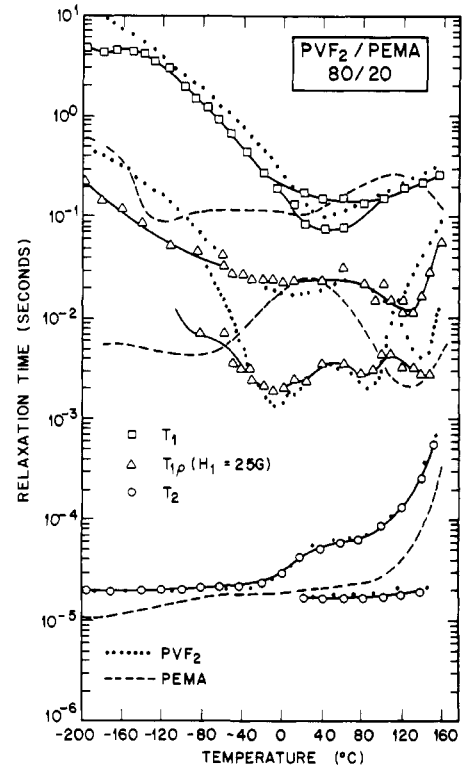


**Figure 12.** $T_1$, $T_2$, and $T_{1\rho}$ data for the 80/20 $PVF_2$/PEMA blend: · · · and - - - denote the $PVF_2$ and PEMA response, respectively.

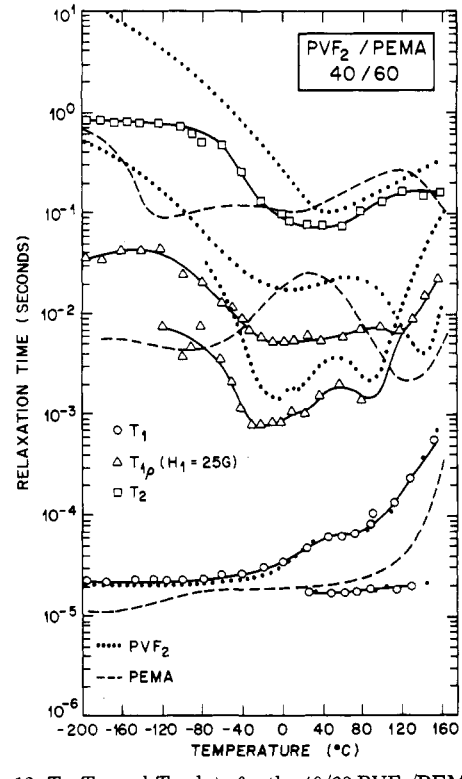


**Figure 13.** $T_1$, $T_2$, and $T_{1\rho}$ data for the 40/60 $PVF_2$/PEMA blend: · · · and - - - denote the $PVF_2$ and PEMA response, respectively.

## Discussion

Cross-relaxation data provide information about the mutual exchange of polarization between spin systems: We recall that

$\sigma$ becomes large when the spectral density function at the difference frequency $J_0(\omega_I - \omega_S)$ becomes large.[11] This is analogous to the development of a $T_{1\rho}$ minimum at the difference frequency for which $\log \nu_C = 6.3$. This expectation is in fact borne out when one compares Figure 6 (or Figure 9) with the corresponding $T_{1\rho}$ data; large cross-relaxation occurs at temperatures somewhat higher than those where $T_{1\rho}$ minima occur, since $(\omega_I - \omega_S)$ is a higher sampling frequency than the one to which the $T_{1\rho}$ data ($H_1 = 25G$) are sensitive. Figures 6 and 9 show that cross-relaxation in the blends displays important differences compared to $PVF_2$. In the vicinity of −40 °C, $\sigma$ increases with PMMA content. This dictates two conclusions, (i) there is increasing intensity in the thermal motion spectrum at the difference frequency $(\gamma_H - \gamma_F)H_0/2\pi = 1.89$ MHz and (ii) this motion directly modulates the proton–fluorine dipole interaction. The fact that the main-chain methyl reorientation in PMMA has a characteristic frequency of ~1.89 MHz at −40 °C makes it the most likely candidate for the modulation motion but one cannot totally disregard the possibility that the presence of the PMMA broadens the spectrum of main chain $PVF_2$ motions responsible for the $\sigma$ peak centered at 0 °C. In either case one is drawn to the conclusion that a substantial fraction of the fluorine nuclei in the amorphous regions has either direct dipole interaction with the PMMA methyl protons or lies on $PVF_2$ molecules with sufficient PMMA near neighbors to alter the main chain $PVF_2$ motions. In other words, a substantial part of the $PVF_2$ molecules "see" PMMA molecules at near neighbor distances. The meaning of the term substantial fraction in this context is difficult to put on a quantitative basis without further experiments on simpler systems. However, an operational definition can be obtained from the data on neat $PVF_2$ which gives a qualitative calibration to the meaning of this phrase.

By definition the cross-relaxation parameter $\sigma$ is the average rate constant, per fluorine nucleus. At −40 °C the dominant contribution to the rate arises from the phonon assisted mutual spin flip and

$$\sigma \approx -\frac{1}{N_I}\sum_{ij}^{N_I N_S} \omega_{0ij}$$

In neat $PVF_2$ the cross-relaxation is chiefly due to modulation of near-neighbor interactions of protons and fluorine by main chain motions at the glass transition. In the blend the observed increase in rate near −40 °C over that in pure $PVF_2$ is approximately one-half the maximum rate observed in pure $PVF_2$. Now $\sigma$ is directly proportional to the number of unlike-spin interactions which are appropriately modulated by molecular motion. Furthermore, $J_0\omega$ for interactions between fluorine nuclei and protons in PMMA is very likely to be larger than the maximum contribution to $J_0\omega$ by near-neighbor protons in $PVF_2$, and therefore one must conclude that the average number of interactions of a fluorine nucleus with PMMA protons must be comparable with the number of proton–fluorine interactions in pure $PVF_2$; a few "points of thermal contact" between the spin systems would lead to an average rate reduced by the ratio of the number of such effective interactions to the total number of possible interactions of unlike spins. On this basis we conclude that at least 20% of the fluorine nuclei "see" near-neighbor PMMA methyl groups. As mentioned above, it is assumed that the $CH_3$ reorientation may be viewed as a local motion which does not propagate in the polymer matrix. Accepting the alternative view that a new distribution of motions is responsible for the stronger cross-relaxation in the blend leaves the conclusion of intimate mixing unchanged.

Examination of the magnitude of the largest spin–lattice transition rate, $\rho$, assigned to the proton spin system, gives support to the notion that the rise in $\sigma$ at −40 °C with increasing PMMA concentration is in fact due to methyl motion. Since the methyl groups provide a large spin–lattice coupling at this temperature one may assume that all of the protons are partially relaxed through spin diffusion to these sinks. Thus the transition rate, as a function of methyl concentration, should be given by $\rho = \rho'_0 3/(8 + 2(n_F/n_H)) + \rho_0$ where $\rho'_0$ is the relaxation rate for a proton on the methyl group, $\rho_0$ is the relaxation rate of a proton on $PVF_2$ in the absence of spin diffusion, and $n_F$ and $n_H$ are the mole fractions of $PVF_2$ and PMMA, respectively. A plot of $\rho$ vs. $3/(8 + 2n_F/n_H)$ for $n_H = 0$, 0.18, and 0.49 gives a straight line, within fairly large experimental error in $\rho$. The slope of this line is in excellent agreement with the transition rate for the main chain methyl in pure PMMA.

In the high-temperature region, above 0 °C, it is observed that cross-relaxation is existent, albeit to varying degrees, up to the melting point of the blends.

It is not expected that there is much cross-relaxation in the crystalline regions of $PVF_2$ since essentially rigid lattice conditions prevail up to the onset of the $\alpha$ relaxation. Referring to the transition map for $PVF_2$,[16] $J_0(\omega_I - \omega_S)$ and therefore $\sigma$ for this relaxation are not expected to be dominant until temperatures in the region of +280 °C which are well outside our range of study. Therefore the observed relaxation effects stem from molecular motions in amorphous material. The striking increase in $\sigma$ with increasing PMMA content at temperatures near +60 °C is almost certainly associated with the transition observed in neat PMMA at this frequency and temperature but not yet identified with a specific molecular motion. This increase like the increase at −40 °C is taken as strong evidence for a substantial degree of intimate mixing of $PVF_2$ and PMMA on a molecular scale in the amorphous phase. In both temperature regions $\sigma$ increases more rapidly than linearly with PMMA concentration. While it may be difficult to model this result, it is consistent with morphological changes, such as lower crystal ordering and more crystal imperfections implied by the high-temperature $T_2$ data.

The larger of the two $\rho$'s for the blends is, at high temperatures, considerably greater than $\rho$ for either pure $PVF_2$ or PMMA (Figures 7 and 10). It would appear that this magnitude of relaxation rate requires that both the PMMA and amorphous $PVF_2$ molecules are undergoing substantial motion at a temperature well below that expected for the glass transition process in pure PMMA.

At low temperatures both $\sigma$ and $\rho$ are small, which does not, however, imply that the ratio $\sigma/\rho$ is small. The question arises as to whether the $^{19}F$ and $^1H$ spin systems are coupled at these temperatures. Although the accuracy of the measurements deteriorates when $\sigma$ and $\rho$ become small, the rise in $\sigma$ at −197 °C in the 75/25 blend may be significant. It may indeed be the remnant of the $\sigma$ peak corresponding to the side chain methyl group motion in PMMA. In the absence of detailed information, however, we can only be guided by the cross-relaxation effects associated with main chain methyl group motion, for which coupling is demonstrated, but one would expect that the spin systems can communicate at the lower temperatures. This would support the earlier contention, based upon $^{19}F$ polarization via main chain $CH_3$ motions, that the two component polymers in the blend are intimately mixed.

Also contained in the cross-relaxation data are the two spin–lattice relaxation times which characterize the observed nonexponential decay predicted by eq 1. These results are compared with the conventionally determined $T_1$ data in Figure 14. Two $T_1$'s are observed over the complete temperature range indicating the greater resolution in the cross-relaxation experiment; this derives from the form of eq 1 which involves the difference of exponentials[11] whereas the usual experiment is described by a sum of exponentials. Where resolution of two $T_1$'s is possible using the 180–90° pulse se-

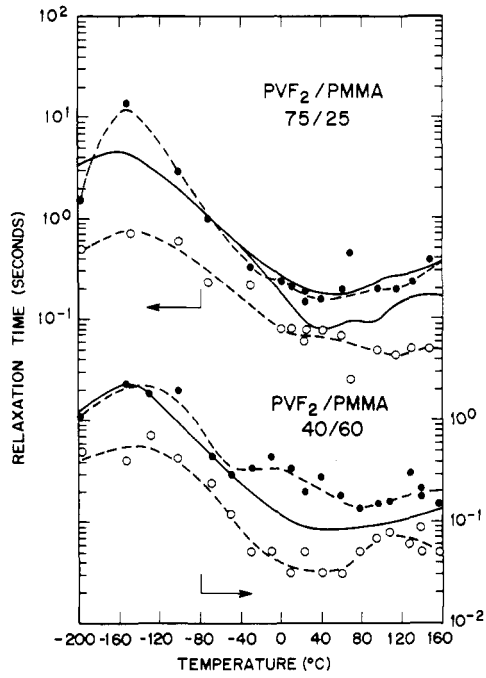


**Figure 14.** Plot of the two component $T_1$'s determined for 1 for the $PVF_2$/PMMA blends as a function of temperature. The solid curves denote the $T_1$ results obtained by conventional pulse methods taken from Figures 5 and 8.

quence, agreement with the cross-polarization results is good. It is noted in passing that this cross-polarization is yet another mechanism, in addition to morphological differences and spin diffusion, which can cause nonexponential decay of magnetization in relatively simple systems.

Turning now to a consideration of the other relaxation data, specifically $T_{1\rho}$ and $T_2$, we again seek evidence of intimate mixing. One might expect $T_2$ in particular to be sensitive to such short-range interactions. Experimentally a small but significant increase in $T_2$ is observed in the blends and one might enquire if this is consistent with intimate mixing.

A rough estimate of $T_2$ for the 75/25 $PVF_2$/PMMA blend may be made on the basis of a simple model in which all the neighboring $PVF_2$ molecules in the amorphous regions are replaced by PMMA molecules. All methyl groups in PMMA are rotating in the selected temperature region of interest, that is, −110 °C. The calculated $^{19}F$ $T_2$ of 22 μs (compared with 20 μs in neat $PVF_2$) provides an upper limit expected for $T_2$ with the addition of the PMMA.

While this increase of 10% in $T_2$ is consistent with observation, it must be concluded that $T_2$ is not a particularly useful or definitive parameter in the characterization of blended polymers such as these. The magnitudes of corresponding $T_1$ and $T_{1\rho}$ minima for the transition associated with the onset of PMMA main chain methyl motion in the blend are computed to be 0.31 and 5.8 ms, respectively. Within the usual constraints in comparing magnitude assessments such as these with experiment data, reasonable agreement is achieved with the $T_{1\rho}$ minimum at −110 °C. No minimum is detected in the data at −30 °C (the temperature at which the appropriate $T_1$ minimum occurs in PMMA) in the directly measured $T_1$ data (Figure 5) but there is evidence of such a minimum in the more sensitive cross-relaxation measurements (Figure 14).

The disappearance of the short $T_2$ component in the blends below the temperature at which this takes place in pure $PVF_2$ is indicative of premelting of the $PVF_2$ crystal regions. The effect is most pronounced in the 40/60 material in which premelting occurs some 60 °C below the melting point of pure $PVF_2$. The $T_{1\rho}$ data support this interpretation with the concurrent disappearance of the crystalline component. This is consistent with the notion that the crystallites formed in the blends are less well ordered or contain more imperfections than their counterparts in pure $PVF_2$.

We have confined our attention so far to the $PVF_2$/PMMA blends for which the most extensive experimental data were available. When the results of Figures 12 and 13 for $PVF_2$/PEMA are compared with their counterparts for $PVF_2$/PMMA (Figures 5 and 8) it is obvious that the relaxation behavior is substantially equivalent in the two types of blend. The general framework of interpretation developed to describe the $PVF_2$/PMMA results is sufficiently flexible as to accommodate the minor variations in detail observed in the $PVF_2$/PEMA. A possible exception to this, however, is the high-temperature behavior of the $T_{1\rho}$ results for the 80/20 $PVF_2$/PMA blend where no crossover point could be established. Instead, the shorter component tends to follow the behavior in PEMA.

## Conclusions

In summary, the main conclusions of this paper are listed as follows:

(i) Cross-relaxation measurements, supported by $T_1$, $T_2$, and $T_{1\rho}$ data, in $PVF_2$/PMMA blends lead to the conclusion that a substantial number of amorphous $PVF_2$ molecules (at least 20% in the 40/60 blend) see PMMA molecules at nearest neighbor distances.

(ii) As in the case of pure $PVF_2$ the fact that $\sigma/\rho$ approaches zero at liquid nitrogen temperature leads to the conclusion that there is little or no cross-relaxation when the lattice is rigid, as is the case for the crystalline portion of $PVF_2$ up to high temperatures.

(iii) The cross-relaxation experiment provides enhanced sensitivity in the measurement of $T_1$ components. This results from the observation of a difference of two exponentials rather than the sum which is the case in the usual $T_1$ experiment.

(iv) There is evidence of extensive premelting of the $PVF_2$ crystallites in the blends.

(v) The NMR behavior of $PVF_2$/PEMA blends is substantially similar to $PVF_2$/PMMA blends.

**Acknowledgments.** We are grateful to Dr. T. K. Kwei for stimulating our interest in blended polymer systems, to Dr. T. T. Wang for his ingenuity in preparing sample materials and much helpful advice, and to Dr. F. A. Bovey for helpful discussions and critical comments on preparation of the manuscript.

## Appendix I

Analysis of cross-relaxation between the hydrogen and fluorine spin systems is based upon a model in which spin diffusion is assumed to be rapid among spins of one species compared to the rate of exchange between unlike species. The equations of motion for the magnetizations are obtained from those derived by Solomon[23] for a single pair of unlike spins through the usual approximation of independent motions which leads to sums of pairwise additive contribution to relaxation. For the

$$\frac{dh_i}{dt} = -\sum_j^{N_I} (\omega_{0ji} + 2\omega_{1ji} + \omega_{2ji})h_i - \sum_j^{N_I} (\omega_{2ji} - \omega_{0ij})f_j - \sum_j^{N_S} (\omega_{0ji} + 2\omega_{1ji} + \omega_{2ji})h_i - \sum_j^{N_S} (\omega_{2ji} - \omega_{0ij})h_j$$

where $h_i = M_{iH}(t) - M_{iH}(0)$, $f_j = M_{iF}(t) - M_{iF}(0)$, and $\omega_{kij}$ is the transition probability with $\Delta m = k$ resulting from interaction between the $i$th and $j$th nuclei. The applicability of Solomon's equations to cross-relaxation in solids is discussed in some measure in ref 11. Rapid spin diffusion within a spin system provides a uniform spin temperature for each species,

or $h_i = h_j$. Summation of the system of eq 1 and their analogue for the fluorine nuclei gives,

$$\frac{dI}{dt} = -\rho(I - I_0) - \frac{N_I}{N_S}\sigma(S - S_0)$$

$$\frac{dS}{dt} = -\rho'(S - S_0) - \sigma(I - I_0)$$

where

$$I = \sum_j M_{jF}(t), \quad S = \sum_j M_{iH}(t)$$

$$\rho = \frac{1}{N_I}\left\{\sum_j^{N_I N_S}(\omega_{0ij} + 2\omega_{1ij} + \omega_{2ij}) + 2\sum_{ij}^{N_S N_S}(\omega_{1ij} + \omega_{2ij})\right\}$$

$$\rho' = \frac{1}{N_S}\left\{\sum_{ij}^{N_I N_S}(\omega_{0ij} + 2\omega_{1ij} + \omega_{2ij}) + 2\sum_{ij}^{N_I N_I}(\omega_{1ij} + \omega_{2ij})\right\}$$

and

$$\sigma = \frac{1}{N_I}\sum_{ij}^{N_I N_S}(\omega_{2ij} - \omega_{0ij})$$

## Appendix II

According to Hamming[24] there is an advantage in monitoring $f(t)$ at equal time intervals $\tau$.

$$f_n(n\tau) = A\left\{e^{-n\alpha_0\tau} - e^{-n\gamma_1\tau}\right\} \tag{A1}$$

where

$$f(t) = \frac{I_z(t) - I_0}{S_0}$$

$$A = 2\sigma/[(\rho' - \rho)^2 + 4\bar{\sigma}^2]^{1/2} \tag{A2}$$

$$\alpha_0 = \tfrac{1}{2}[\rho + \rho' + [(\rho - \rho')^2 + 4\bar{\sigma}^2]^{1/2}]$$

$$\alpha_1 = \tfrac{1}{2}[\rho + \rho' - [(\rho - \rho')^2 + 4\bar{\sigma}^2]^{1/2}]$$

$$\bar{\sigma} = [N_F/N_H]^{1/2}\sigma$$

The $f_n$ satisfy the following recursion formula

$$f_n + C_1 f_{n+1} + C_2 f_{n+2} = 0 \tag{A3}$$

Therefore, using the minimum number of sampling points, 3, gives

$$C_1 = \frac{-f_0 f_3 + f_1 f_2}{f_1 f_3 - f_2^2} \qquad C_2 = \frac{-f_1^2 + f_0 f_2}{f_1 f_3 - f_2^2} \tag{A4}$$

Again following Hamming, the eigenvalue equation associated with (A3) is

$$\rho^2 + C_1\rho + C_2 = 0 \tag{A5}$$

where the eigenvalues $\rho_\pm$ are

$$\rho_\pm = \frac{-C_1 \pm [C_1^2 - 4C_2]^{1/2}}{2} \tag{A6}$$

and

$$\alpha_0 = -\frac{1}{\tau}\ln \rho_+$$

$$\alpha_1 = -\frac{1}{\tau}\ln \rho_-$$

$$A = \frac{f_1\rho_+\rho_-}{\rho_- - \rho_+} \tag{A7}$$

Substituting these values for $\alpha_0$, $\alpha_1$, and $A$ into A2 provides $\sigma$, $\rho$, and $\rho'$.

## References and Notes


(1) L. Bohn, *Kollid Ż. Z. Polym.*, **213**, 55 (1966).
(2) S. Krause, *J. Macromol. Sci., Rev. Macromol. Chem.*, **7**, 251, (1972).
(3) M. Bank, J. Leffingwall, and C. Thies, *Macromolecules*, **4**, 43 (1971); *J.Polym. Sci., Part A-2*, **10**, 1097 (1972).
(4) L. P. McMaster, *Macromolecules*, **6**, 760 (1973).
(5) D. R. Paul and J. O. Altamirano, *Polym. Prepr., Am. Chem. Soc., Div. Polym. Chem.*, **15**, 409 (1974).
(6) J. W. Schurer, A. deBoer, and G. Challa, *Polymer*, **16**, 201 (1975).
(7) T. Nishi, T. T. Wang, and T. K. Kwei, *Macromolecules*, **8**, 227 (1975).
(8) T. Nishi and T. K. Kwei, *Polymer*, **16**, 285 (1975).
(9) T. Nishi, T. K. Kwei, and T. T. Wang, *J.Appl. Phys.*, **46**, 4157 (1975).
(10) T. K. Kwei, T. Nishi, and R. F. Roberts, *Macromolecules*, **7**, 667 (1974).
(11) V. J. McBrierty and D. C. Douglass, *Macromolecules*, **10**, 855 (1977).
(12) T. Nishi and T. T. Wang, *Macromolecules*, **8**, 909 (1975).
(13) G. D. Patterson, T. Nishi, and T. T. Wang, *Macromolecules*, **9**, 603 (1976).
(14) J. S. Noland, N. N. C. Hsu, R. Saxon, and J. M. Schmitt *Adv. Chem. Ser.*, **No. 99**, 15 (1971).
(15) D. W. McCall, *Natl. Bur. Stand. (U.S.), Spec. Publ.*, **No. 310**, 475 (1969).
(16) V. J. McBrierty, D. C. Douglass, and T. A. Weber, *J. Polym. Sci., Polym. Phys. Ed.*, **14**, 1271 (1976).
(17) P. J. Flory, "Principles of Polymer Chemistry", Cornell University Press, Ithaca, N.Y., 1953.
(18) G. P. Jones, D. C. Douglass, and D. W. McCall, *Rev. Sci. Instrum.*, **36**, 1461 (1965).
(19) J. G. Powles and P. Mansfield, *Phys. Lett.*, **2**, 58 (1962).
(20) G. E. Wardell and V. J. McBrierty, *Proc. R. Irish Acad.*, **73**, 63 (1973).
(21) H. Y. Carr and E. M. Purcell, *Phys. Rev.*, **94**, 630 (1954).
(22) S. R. Hartmann and E. L. Hahn, *Phys. Rev.*, **128**, 2042 (1962).
(23) I. Solomon, *Phys. Rev.*, **99**, 559 (1955).
(24) R. Hamming, "Numerical Methods for Scientists and Engineers", McGraw-Hill, New York, N.Y., 1962, p 338 ff.
(25) W. P. Slichter, *J. Polym. Sci., Part C*, **14**, 33 (1966).